

Figure S1. Related to Figure 1.

- (A) Imagestream analysis of nuclear localization of pSTAT1 following IFN treatment. PH5CH8 cells were treated with 25 IU/ml IFNβ or 100 ng/ml IFNλ3 for 30 mins.
- (B) Representative histogram of pSTAT1 nuclear localization in IFN-treated cells.
- (C) Analysis of transcription factor binding sites in ISG15 promoter. Highlighted are IRF1 and STAT binding sites as well as the EMSA probe sequence.
- (D) Supershift assay using nuclear extracts from cells treated with IFNβ (125 IU/ml) or IFNλ3 (500ng/ml) for 1h co-incubated with antibodies against the indicated proteins.
- (E) Representative UV spectra from polysome sedimentation of PH5CH8 cells stimulated with IFN for the indicated time.
- (F) Changes in ISG15, OAS1, and CXCL10 mRNA expression at 8, 24, 36h of treatment with IFN relative to untreated cells. All data is representative of 3 or more experiments, unless otherwise stated.

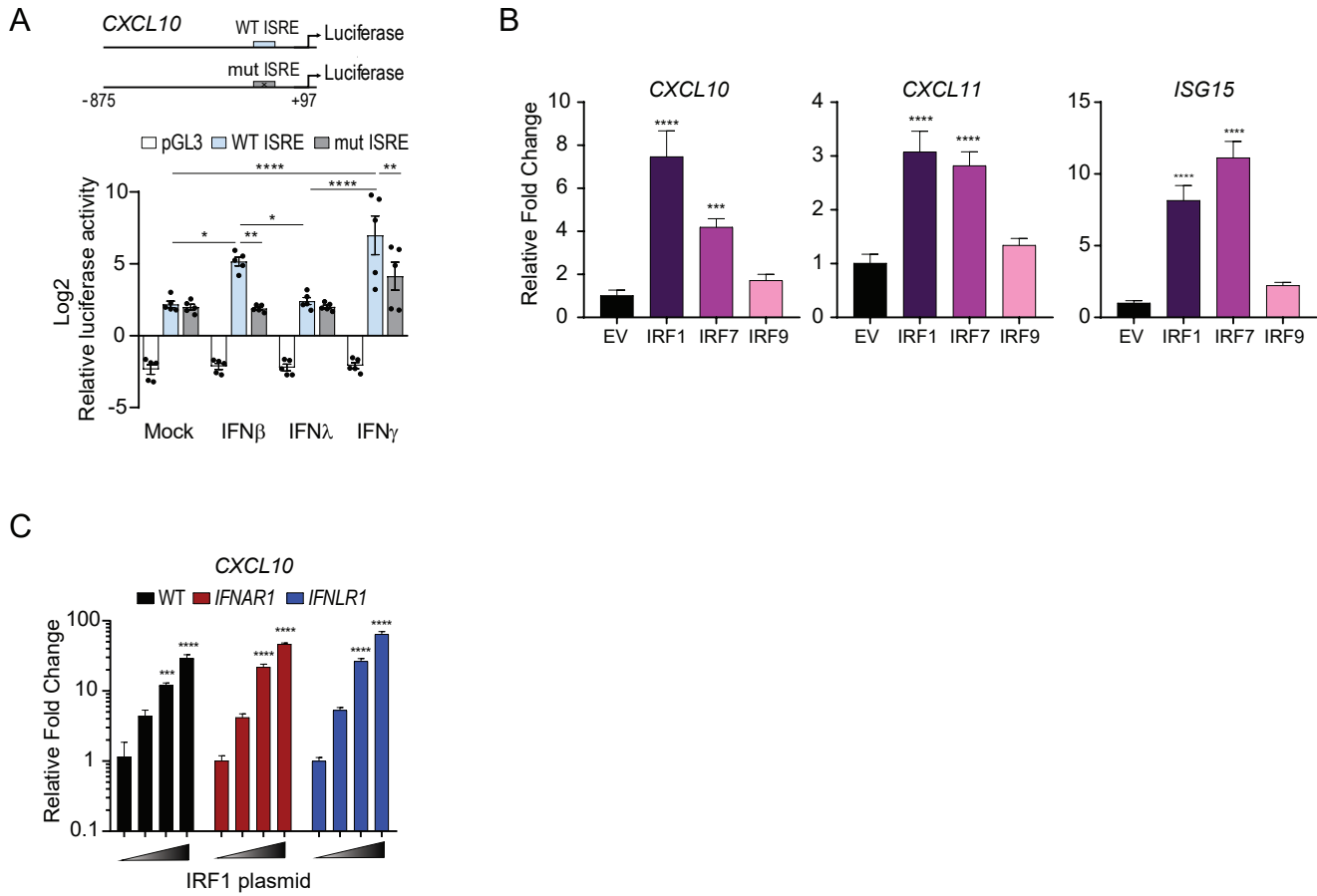


Figure S2. Related to Figure 2.

(A) Firefly luciferase activity of WT CXCL10 and mutant ISRE CXCL10 promoter following 6h of treatment with IFN β (1000 IU/ml), IFN λ (100 ng/ml), or IFN γ and TNF α (20 ng/ml each). Bar graph represents an average of 5 independent experiments. Statistical significance was determined using two-way ANOVA.

(B) Exogenous IRF1 expression is sufficient for the induction of CXCL10 and ISG15 in 2fTGH cells. Statistical significance was determined using one-way ANOVA.

(C) qPCR analysis of CXCL10 mRNA following transfection with 100, 250, and 500 ng of IRF1 expression vector or empty vector in Huh7 WT, IFNAR-deficient and IFNLR1-deficient cells.

Relative changes in expression were normalized to genotyped-matched empty vector-transfected cells and HPRT. Unless otherwise indicated, data presented is representative of three independent experiments. Asterisk (*) denote p-values <0.05.

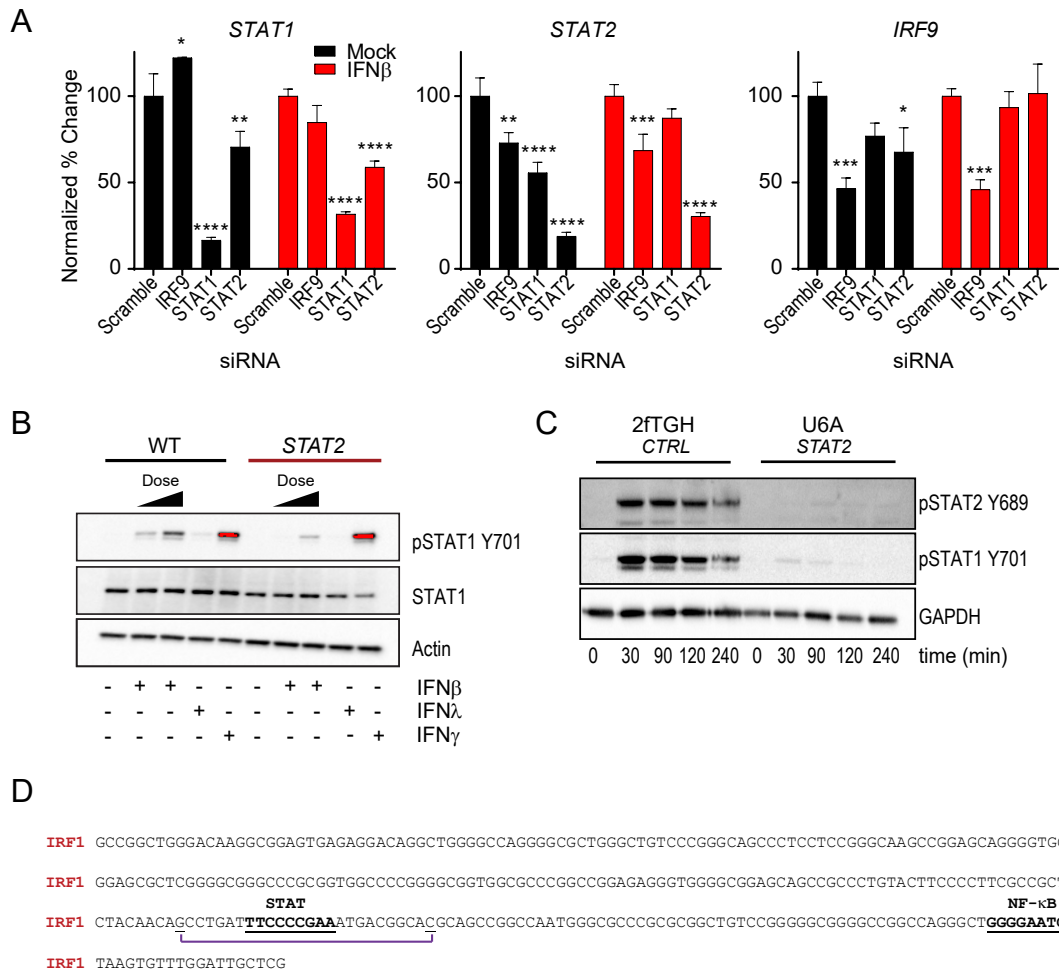


Figure S3. Related to Figure 3.

(A) qPCR analysis of *STAT1*, *STAT2*, and *IRF9* mRNA following siRNA transfection as indicated as indicated in Figure 3A. Changes in the percent of mRNA expression is represented relative to those of control siRNA transfected cells (100%) and normalized to *HPRT*.

(B) Immunoblot analysis of pSTAT1 (Y701), STAT1, and β-Actin in WT and STAT2 KO PH5CH8 cells treated with IFNβ (25 IU/ml or 250IU/ml), IFNλ3 (100 ng/ml), or IFNγ (5ng/ml) for 90 min. Red indicates saturated pixels.

(C) Immuno blot analysis of phosphorylated STAT1 (Y701) and STAT2 (Y689) following IFNβ treatment of 2fTGH, U3A, and U6A cells for the indicated timepoints.

(D) IRF1 promoter sequence analysis. Highlighted are STAT and NF-κB binding sites as well as the EMSA probe (purple). Unless otherwise indicated, data presented is representative of three independent experiments. Asterisk (*) denote p-values <0.05.

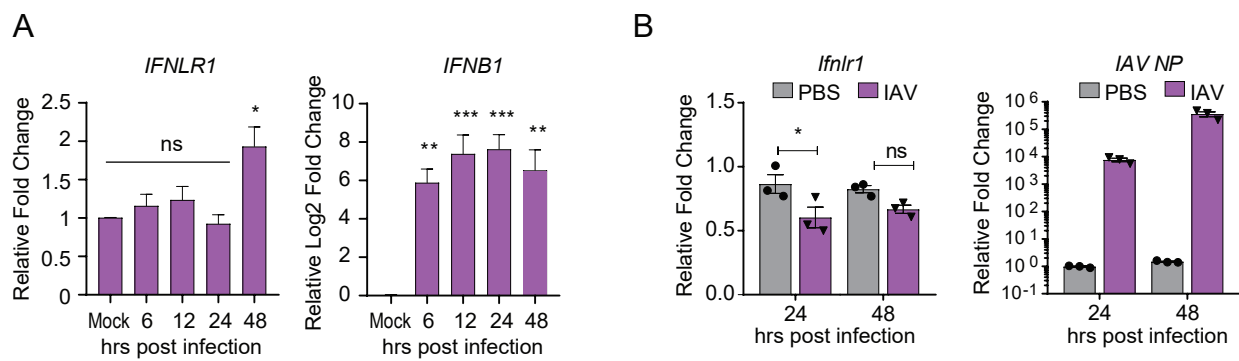


Figure S4. Related to Figure 4.

(A) qPCR analysis of *IFNLR1* and *IFNB1* mRNA in A549 cells infected with IAV (A/CA/04/2009) at an moi=1. Gene expression was normalized relative to HPRT. Statistical significance was determined using one-way ANOVA.

(B) qPCR analysis of the average (n=3) expression of *Ifnlr1* mRNA in whole lungs after infection with IAV (A/PR/8/34) at the indicated timepoints relative to *Gapdh*. IAV NP expression was determined relative to Chmp2a and PBS treated lungs (value 1). Statistical significance was determined using two-way ANOVA.

Unless otherwise indicated, data represents mean \pm SEM across 3 independent experiments. Asterisk (*) denote p-values <0.05.

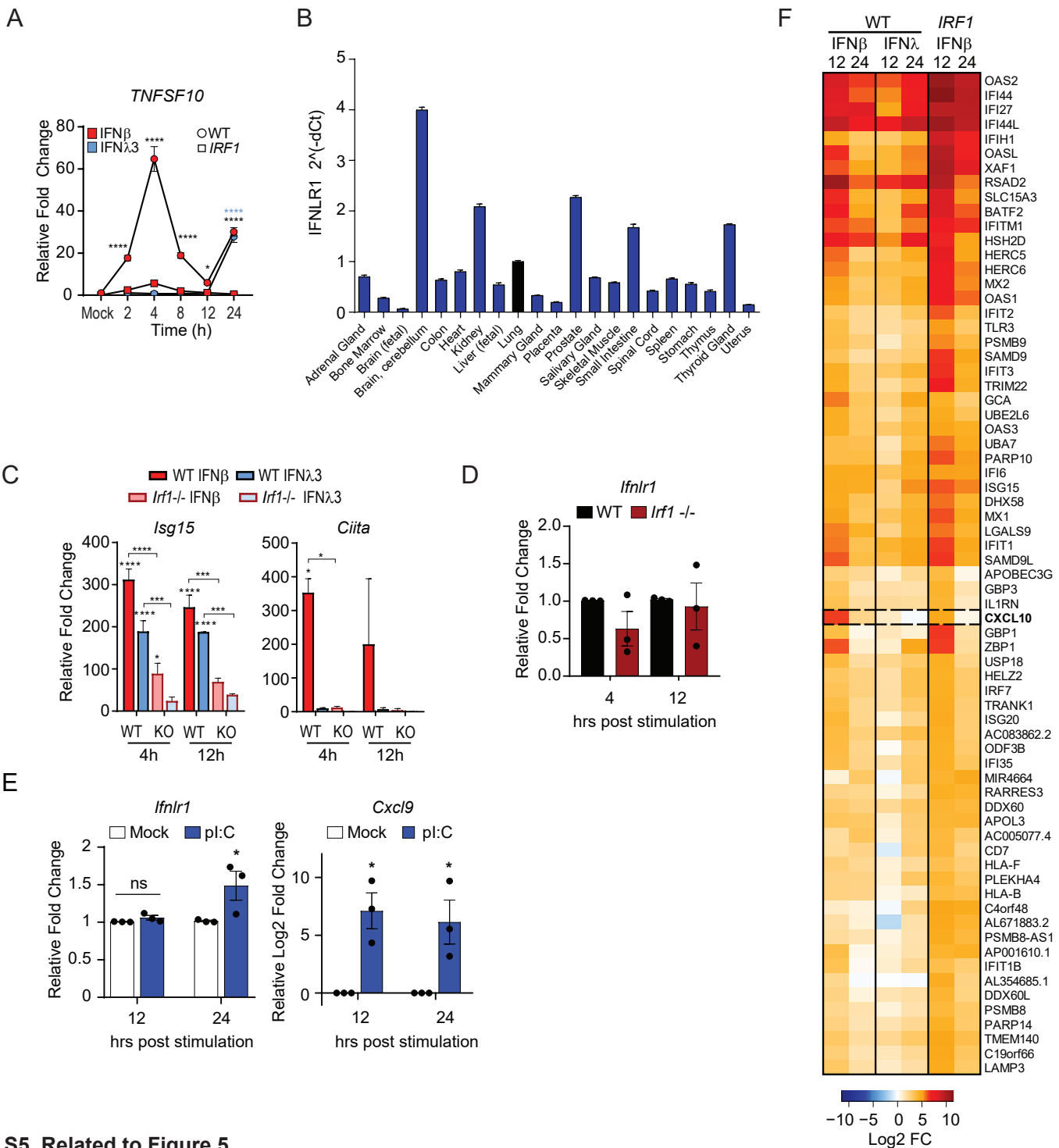


Figure S5. Related to Figure 5.

- (A) qPCR analysis of *TNFSF10* after IFN β (25IU/ml) or IFN λ 3 (100 ng/ml) treatment for the indicated times in WT (circle) or IRF1-deficient cells (square). Relative mean \pm SEM mRNA expression was determined relative to *HPRT* and non-stimulated controls.
- (B) Relative mean \pm SD *IFNLR1* mRNA expression normalized to lung (relative value=1; Black bars).
- (C) qPCR analysis of *Isg15* and *Ciita* mRNA in WT and *Irf1*-/- small intestinal organoids treated with murine IFN β or IFN λ 3 for the indicated timepoints. Relative mean \pm SD mRNA expression is normalized to *Actin* control.
- (D) qPCR analysis of basal *Ifnlr1* mRNA expression in WT and *Irf1*-/-small intestinal organoids. Relative mean \pm SD mRNA expression was normalized to *Gapdh* and time-matched WT organoid samples.
- (E) qPCR analysis of mean \pm SEM *Ifnlr1* and *Cxcl9* mRNA expression following poly I:C stimulation (2ug/ml) of primary small intestinal epithelial cells. Relative mRNA expression was normalized to *Gapdh* and time-matched mock-treated cells.
- (F) Heatmap of the relative expression of 69 transcripts identified in the Cluster VI (Cyan). Unless otherwise indicated, data presented is representative of three independent experiments. Asterisk (*) denote p-values <0.05 .

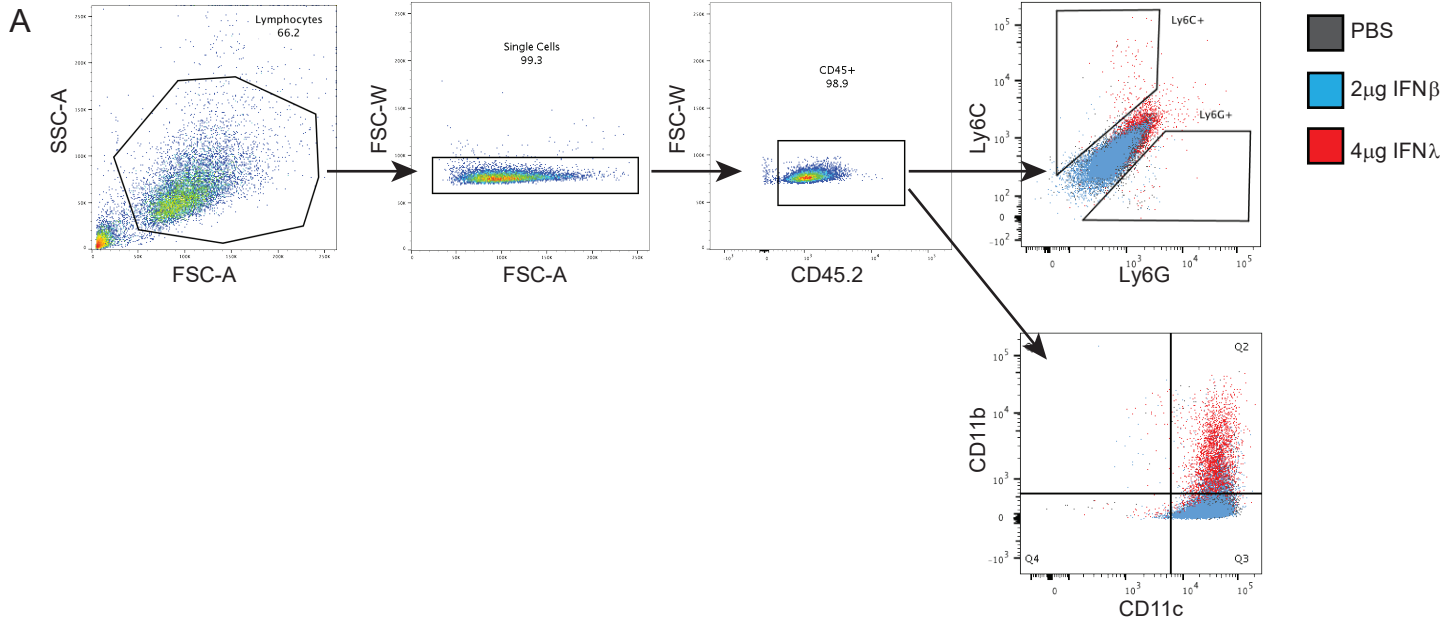


Figure S6. Related to Figure 6.

(A) Schematic representation of the gating strategy used to identify cellular infiltrate in the BAL from IFN-inoculated mice.

Table S1. Related to Figure 4.

Module	# Genes	Canonical Pathways	p-value
Red - I	502	SAPK/JNK signaling	6.81E-05
		Germ cell-Sertoli cell junction signaling	3.09E-04
		Sirtuin signaling pathway	1.39E-03
		Axonal guidance signaling	1.57E-03
		Integrin signaling	2.40E-03
Yellow - II	222	Intrinsic Prothrombin activation pathway	5.00E-03
		Retinol biosynthesis	5.00E-03
		IL-15 production	2.22E-02
		L-serine degradation	2.45E-02
		GP6 signaling pathway	2.51E-02
Skyblue - III	268	Antigen presentation pathway	3.79E-08
		Interferon signaling	6.90E-07
		Activation of IRF by cytosolic PRR	2.38E-04
		Complement system	3.11E-04
		Dendritic cell maturation	1.74E-03
Black - IV	195	Neurorotective Role of THOP1 in Alzheimer's Disease	6.94E-04
		Inflammasome pathway	6.08E-03
		TREM1 signaling	9.85E-03
		Altered T and B cell signaling in RA	1.61E-02
		Communication between innate and adaptive immune cells	1.86E-02
Blue - V	685	IL-22 signaling	3.96E-04
		Coagulation system	2.37E-03
		Amyloid processing	2.46E-03
		RhoGDI signaling	3.27E-03
		Sertoli cell-Sertoli cell junction signaling	3.43E-03
Cyan - VI	69	Interferon signaling	4.05E-16
		Activation IRF by cytosolic PRR	1.94E-08
		Role PRR in recognition of bacteria and viruses	2.01E-06
		Antigen Presentation Pathways	3.48E-06
		Communication between innate and adaptive immune cells	6.18E-06
DarkBlue - VII	132	Putrescine biosynthesis III	3.91E-03
		Creatine-phosphate biosynthesis	9.76E-03
		Synaptic long term potentiation	2.39E-02
		RhoA signaling	2.46E-02
		Cellular effects of Sildenafil	2.72E-02
DarkRed - VIII	56	Glycoaminoglycan-protein linkage region biosynthesis	3.19E-03
		Chondroitin Sulfate biosynthesis	2.57E-02
		Dematan Sulfate biosynthesis	2.66E-02
		Heparan Sulfate biosynthesis	3.67E-02
		Iron homeostasis signaling pathway	5.90E-02
Orange - IX	273	Glucocorticoid Receptor Signaling	1.12E-04
		Role of osteoblasts, osteoclasts and chondrocytes in RA	3.15E-04
		Atherosclerosis signaling	6.98E-04
		Airway pathology in COPD	8.26E-04
		Psteoarthritis pathway	1.16E-03